A 50 GHz SiGe BiCMOS Active Bandpass Filter

Saurabh Chaturvedi, *Member, IEEE*, Mladen Božanić, *Senior Member, IEEE*,
and Saurabh Sinha, *Senior Member, IEEE*

Department of Electrical and Electronic Engineering Science, Faculty of Engineering and the Built Environment
University of Johannesburg, Auckland Park Kingsway Campus
Johannesburg, South Africa
E-mail: chaturvedi.s.in@ieee.org, mbozanic@ieee.org, ssinha@ieee.org

***Abstract* - This paper presents a second-order active bandpass filter (BPF) at millimeter-wave frequency band using 0.13 μm SiGe BiCMOS technology. A complementary cross-coupled pair based negative resistance technique is applied to compensate for the resistive losses of microstrip line resonators. The proposed active BPF is simulated using the Keysight Technologies (formerly Agilent's Electronic Measurement Group) Advanced Design System 2016.01. The center frequency (f_c), 3-dB bandwidth, and fractional bandwidth of the simulated BPF are 53.85 GHz, 14.18 GHz, and 26.33%, respectively. The BPF shows an insertion loss (IL) of 0.33 dB and a return loss (RL) of 18.03 dB at f_c. The minimum IL of 0.10 dB and best RL of 26.03 dB are observed in the passband. The noise figure and input 1-dB compression point (P_{1dB}) at f_c are 7.93 dB and -3.67 dBm, respectively. The power dissipation is 2.62 mW at 1.6 V supply voltage. For the input power level of -10 dBm, the power level of the second harmonic is -46.02 dBc.**

***Keywords* - Bandpass filter (BPF), SiGe BiCMOS, negative resistance, loss compensation, resonator, process design kit (PDK).**

I. INTRODUCTION

The operating frequencies of wireless communication systems have increased rapidly with the continuous growth in communication technology. Owing to the development of millimeter-wave (mm-wave) transceivers, high-speed data transfer through wireless local area networks, wireless home networks, and wireless personal area networks is possible [1]. In these communication systems, filters are essential front-end components for signal selection at specific frequencies. Their electrical responses are critical for the overall system performance.

suffer from the prime disadvantage of high loss. Active devices are used to compensate for the losses of passive resonators and to improve their quality factors (Q-factors). By applying loss compensation (Q-enhancement) techniques, active BPFs are realized and can be used in a transceiver module for reducing the loss and size [2]. Passive BPFs also have the shortcomings of incompatibility with tunable elements, trade-off between bandwidth (BW) and insertion loss (IL), and low out-of-band rejection levels. The Q-factor of a monolithic transmission line (TL) is directly proportional to the square root of the frequency of operation. Thus, with increasing frequencies, the Q-factor of a TL is enhanced. Consequently, TLs are broadly used and preferred as resonators for mm-wave filter design [3].

In this paper, complementary MOS cross-coupled pair loss compensation topology is used to enhance the Q-factor of a microstrip TL resonator. The proposed active BPF implemented using the GlobalFoundries 0.13 μm SiGe BiCMOS8HP process design kit (PDK) exhibits excellent performance.

The rest of the paper is organized as follows: Section II discusses the Q-enhanced microstrip TL resonator using a complementary cross-coupled pair and its equivalent circuit model. Section III illustrates the schematic diagram of the second-order active BPF with Q-enhanced TL resonators and provides the details of PDK models of the GlobalFoundries BiCMOS8HP technology used. Simulation results of the implemented active BPF with a performance comparison table are presented in Section IV. The paper is concluded in Section V.

II. Q-ENHANCED TL RESONATOR

The schematic of the Q-enhanced microstrip line resonator using a complementary cross-coupled pair is shown in Fig. 1, and Fig. 2 presents its equivalent circuit model. In the complementary cross-coupled pair configuration, the negative conductances $-G_N$ and $-G_P$ are provided by NMOS and PMOS transistors, respectively. These negative conductances are produced with differential excitation and serve to compensate for the resistive losses of the passive resonator. L_{eq}, C_{eq}, and G_{eq} denote the equivalent inductance, capacitance, and conductance [4]. The expressions of G_{eq} and C_{eq} are given by (1) and (2), respectively. α, l, and Y_c are the attenuation constant, length, and characteristic admittance of the TL, respectively [4].

$$G_{eq} = Y_c \alpha l \tag{1}$$

$$C_{eq} = \frac{\pi Y_c}{2\omega_0} \tag{2}$$

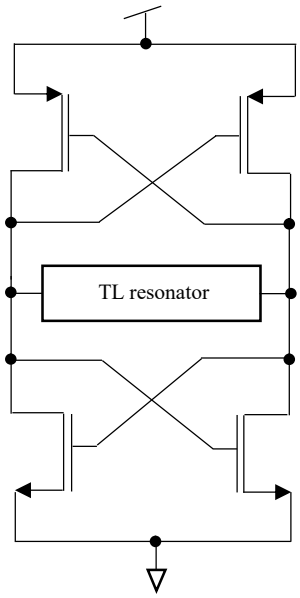

Fig. 1. Schematic of *Q*-enhanced resonator.

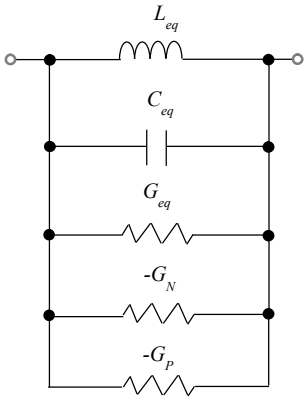

Fig. 2. Equivalent lumped circuit model.

The expression of the total *Q*-factor (Q_t) of the *Q*-enhanced resonator is given by (3).

$$Q_t = \frac{\omega_0 C_{eq}}{G_{eq} - (G_N + G_P)} \tag{3}$$

Using (1) and (2) in (3), Q_t can be represented by (4),

$$Q_t = \frac{\pi}{2\left[\alpha l - Z_c (G_N + G_P)\right]} \tag{4}$$

where Z_c is the characteristic impedance of the TL.

III. ACTIVE BPF

Fig. 3 demonstrates the schematic diagram of the second-order active BPF with *Q*-enhanced TL resonators.

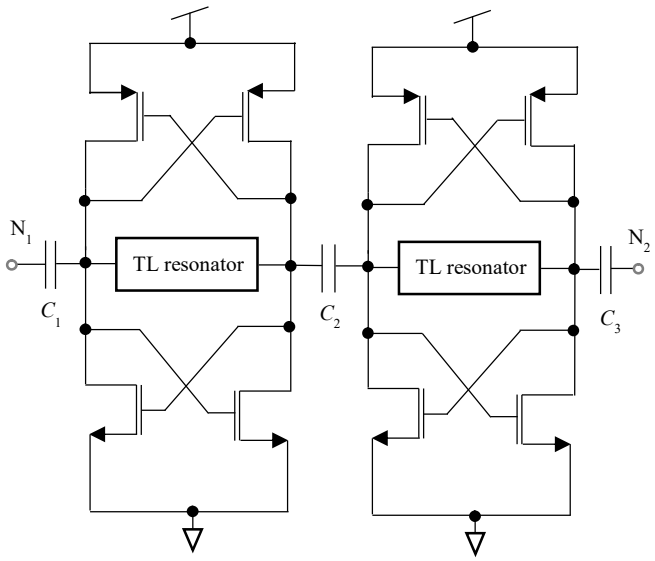

Fig. 3. Schematic of active BPF.

GlobalFoundries 0.13 μm SiGe BiCMOS8HP technology [5] offers three back end of line (BEOL) metallization options, including seven levels of metal (7LM), six levels of metal (6LM), and five levels of metal (5LM). In this work, the 5LM option is selected, which consists of two thin copper layers, M1 and M2, one thick copper layer, MQ, and two thick aluminium layers, LY and AM. The resistivity of the silicon substrate is 11-16 Ω-cm and the maximum power supply voltage for the thin gate oxide MOSFETs is 1.6 V. The thin gate oxide FET PDK models, nfet and pfet, are used. The minimum channel width and length of these MOSFET devices are 0.16 μm and 0.12 μm, respectively.

In the BiCMOS8HP PDK, the model singlewire is a microstrip TL structure that incorporates one signal line, a metal ground plane, and optional side shields. The BEOL metal levels for the signal line and ground plane are chosen by the designer. In the proposed active BPF, the metal layers, AM and M1, are used as signal line and ground plane, respectively. The width of the ground plane is a function of the model input parameters and is limited by the maximum allowed width of the ground plane metal layer. The length and width of the singlewire microstrip TLs used in this BPF implementation are 640 μm and 9 μm, respectively.

The BiCMOS8HP technology provides three types of capacitors: MOS varactor, hyper abrupt junction diode varactor (HA varactor), and single aluminium metal-insulator-metal (MIM) capacitor. The PDK model, mim, is used for the MIM capacitor in this filter design. The values of C_1, C_2, and C_3 MIM capacitors in Fig. 3 are 50 fF, 17 fF, and 50 fF, respectively.

IV. SIMULATION RESULTS

Figs. 4(a, b) present the simulated frequency responses of the active BPF using the Keysight Advanced Design System (ADS) 2016.01. The center frequency (f_c), 3-dB BW, and fractional BW (FBW) of the simulated BPF are 53.85 GHz, 14.18 GHz, and 26.33%, respectively. The BPF shows an IL of 0.33 dB and a return loss (RL) of 18.03 dB at f_c. The minimum IL of 0.10 dB and best RL of 26.03 dB are observed in the passband.

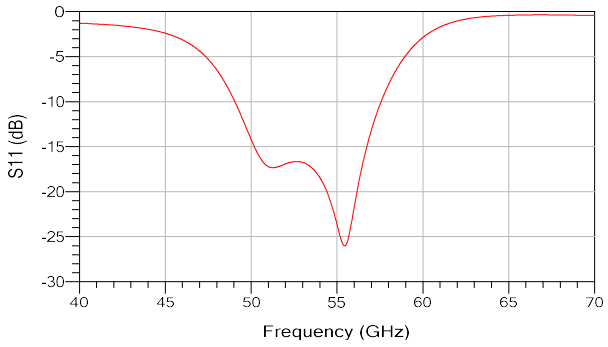

(a)

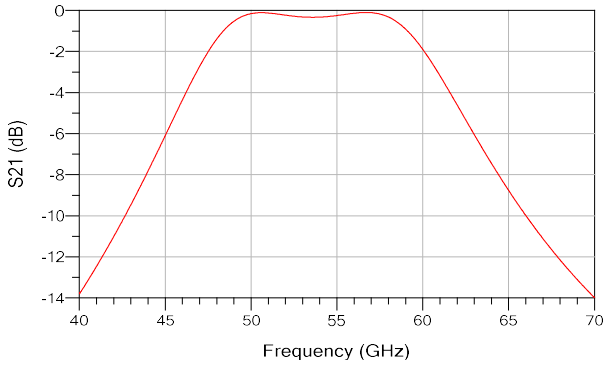

(b)

Fig. 4. Frequency responses.

The variation of the noise figure (NF) with frequency is depicted in Fig. 5. The NF value at f_c is 7.93 dB. The gain against input power (P_{in}) is plotted in Fig. 6. The input 1-dB compression point (P_{1dB}) at f_c is -3.67 dBm.

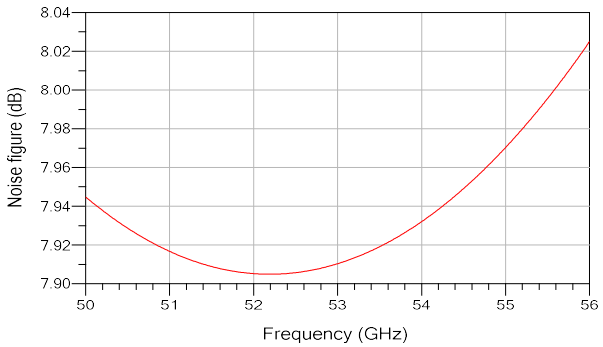

Fig. 5. NF vs frequency plot.

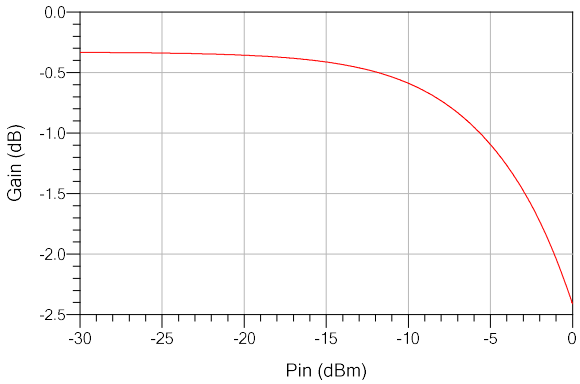

Fig. 6. Gain vs P_{in} plot.

Fig. 7 illustrates the power levels of the fundamental frequency and second harmonic. For -10 dBm of input power level, the power levels of the fundamental frequency and second harmonic are -10.59 dBm and -56.61 dBm, respectively. Therefore, the difference between their power levels is 46.02 dB. The DC power dissipation (P_{DC}) of the BPF is 2.62 mW at 1.6 V supply voltage.

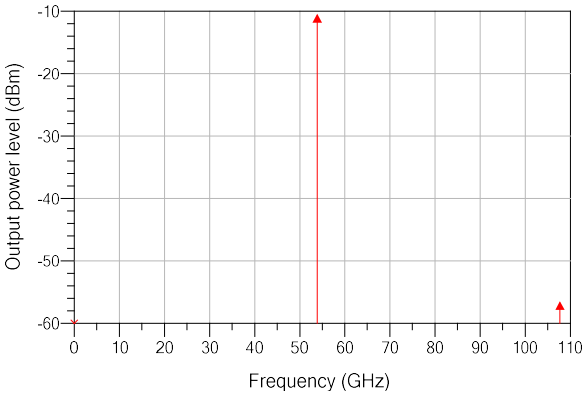

Fig. 7. Output power level vs frequency plot.

Table I compares the performance of the implemented active BPF with the previously published active BPFs.

The parameter figure of merit (FOM) is defined by (5) [7],

$$\mathrm{FOM_{dB}} = 10\log\left(\frac{N \times \mathrm{P_{1dB}} \times f_c}{\mathrm{FBW} \times \mathrm{P_{DC}} \times \mathrm{NF}}\right) \quad (5)$$

where P_{DC} and P_{1dB} are in W, and f_c is in Hz. NF is used in the form of a noise factor (not converted to dB), and FBW is the ratio of 3-dB BW to f_c (not converted to percentage).

TABLE I. PERFORMANCE COMPARISON OF ACTIVE BPFs

Ref.	Process	Order (N)	f_c (GHz)	FBW (%)	P_{DC} (mW)	NF (dB)	P_{1dB} (dBm)	IL (dB)	RL (dB)	FOM (dB)
[6]	0.15 μm GaAs	2	22.6	4	50.4	17	-19	8	7.7	67.5
[3]	0.18 μm CMOS	2	34.2	18.8	3.7	7*	-4.6	0	14.6	98.3
[4]	0.18 μm CMOS	2	22.7	7.39	3.3	14.05	-7.7	0.15	9.96	91
[7]	0.18 μm CMOS	2	23.5	17	4.2	6.7	-3.5	1.65	13.2	98
[8]	0.18 μm CMOS	2	2.44	2.46	10.8	18	-15	6	19	70
[9]	0.18 μm CMOS	2	6.02	18.94	5.4	12	-15.2	2.2	7.64	73.5
[10]	0.13 μm CMOS	2	24.1	3.86	5.4	14.05	-25.43	0	13.3	74
[11]	0.18 μm CMOS	2	5.3	32	2.2	4.3	2.5	0.77	18	100
[2]	0.15 μm GaAs	2	65	4	-	10.5	-	3	9.4	-
[2]	0.15 μm GaAs	2	65	2	-	-	5	2.8	9.1	-
This work*	0.13 μm SiGe BiCMOS	2	53.85	26.33	2.62	7.93	-3.67	0.33	18.03	100.33

* Simulated results

V. CONCLUSION

A second-order 0.13 μm SiGe BiCMOS mm-wave active BPF with f_c of 53.85 GHz is reported in this article. The complementary cross-coupled pair configuration is used to compensate for the losses of TL resonators. ADS simulation results of the proposed active BPF show excellent filter performance. The performance comparison table reveals that the FOM of this implemented active BPF is higher than the previously published active BPFs.

ACKNOWLEDGMENT

The authors would like to thank Dr Valentin Buiculescu of IMT Bucharest, Romania for the useful discussions and comments.

REFERENCES

[1] S. Singh, F. Ziliotto, U. Madhow, E. Belding, and M. Rodwell, "Blockage and directivity in 60 GHz wireless personal area networks: from cross-layer model to multihop MAC design," *IEEE J. Sel. Areas Commun.*, vol. 27, no. 8, pp. 1400-1413, Oct. 2009.

[2] M. Ito, K. Maruhashi, S. Kishimoto, and K. Ohata, "60-GHz-band coplanar MMIC active filters," *IEEE Trans. Microw. Theory Tech.*, vol. 52, no. 3, pp. 743-750, Mar. 2004.

[3] M.-J. Chiang, H.-S. Wu, and C.-K. C. Tzuang, "A 3.7-mW zero-dB fully integrated active bandpass filter at Ka-band in 0.18-μm CMOS," in *Proc. IEEE MTT-S Int. Microw. Symp.*, 2008, pp. 1043-1046.

[4] K.-K. Huang, M.-J. Chiang, and C.-K. C. Tzuang, "A 3.3 mW K-band 0.18-μm 1P6M CMOS active bandpass filter using complementary current-reuse pair," *IEEE Microw. Wireless Compon. Lett.*, vol. 18, no. 2, pp. 94-96, Feb. 2008.

[5] MOSIS Integrated Circuit Fabrication Service. [Online]. Available: https://www.mosis.com

[6] K.-W. Fan, C.-C. Weng, Z.-M. Tsai, H. Wang, and S.-K. Jeng, "K-band MMIC active band-pass filters," *IEEE Microw. Wireless Compon. Lett.*, vol. 15, no. 1, pp. 19-21, Jan. 2005.

[7] S. Wang and B.-Z. Huang, "Design of low-loss and highly-selective CMOS active bandpass filter at K-band," *Progress Electromag. Research*, vol. 128, pp. 331-346, Jun. 2012.

[8] Z. Gao, J. Ma, M. Yu, and Y. Ye, "A fully integrated CMOS active bandpass filter for multiband RF front-ends," *IEEE Trans. Circuits Syst.-II: Express Briefs*, vol. 55, no. 8, pp. 718-722, Aug. 2008.

[9] C.-K. C. Tzuang, H.-H. Wu, H.-S. Wu, and J. Chen, "CMOS active bandpass filter using compacted synthetic quasi-TEM lines at C-band," *IEEE Trans. Microw. Theory Tech.*, vol. 54, no. 12, pp. 4548-4555, Dec. 2006.

[10] L. Su and C.-K. C. Tzuang, "A narrowband CMOS ring resonator dual-mode active bandpass filter with edge periphery of 2% free-space wavelength," *IEEE Trans. Microw. Theory Tech.*, vol. 60, no. 6, pp. 1605-1616, Jun. 2012.

[11] S. Wang and W.-J. Lin, "C-band complementary metal-oxide-semiconductor bandpass filter using active capacitance circuit," *IET Microw. Antennas Propag.*, vol. 8, no. 15, pp. 1416-1422, Dec. 2014.